Respiratory Motion Correction in 4D PET/CT: Comparison of Implementation Methodologies for Incorporation of Elastic Transformations in the Reconstruction System Matrix

F. Lamare*, M.J. Ledesma Carbayo†, A.J. Reader‡, O.R. Mawlawi§, G. Kontaxakis†, A. Santos†, C. Cheze-Le Rest*, D. Visvikis*

*U650 INSERM, Laboratoire du traitement de l'information médicale (LaTIM), Université de Bretagne occidentale, Brest, France
†ETSI Telecomunicacion Universidad Politecnica de Madrid, Ciudad Universitaria s/n 28040, Madrid, Spain
‡Department of Instrumentation and Analytical Science, UMIST, Manchester, UK
§University of Texas M.D. Anderson Cancer Center, Houston, United States

Abstract— **Respiratory motion in emission tomography leads to reduced image quality. Proposed correction methodology has been concentrating on the use of respiratory synchronised acquisitions leading to gated frames. Such frames however are of low signal to noise ratio as a result of containing reduced statistics. Therefore a method accounting for respiratory motion effects without affecting the statistical quality of the reconstructed images is necessary. In this work we describe the implementation of an elastic transformation within a list-mode based reconstruction for the correction of respiratory motion over the thorax. The developed algorithm was evaluated using datasets of the NCAT phantom generated at different points throughout the respiratory cycle. List mode data based PET simulated frames were subsequently produced by combining the NCAT datasets with a Monte Carlo simulation. Transformation parameters accounting for respiratory motion were estimated according to an elastic registration of the NCAT dynamic CT images and were subsequently applied during the image reconstruction of the original emission list mode data. The One-pass list mode EM (OPL-EM) algorithm was modified to integrate the elastic transformation in the sensitivity matrix. Three different implementations have been investigated (no interpolation, trilinear interpolation, b-spline functions incorporation). The corrected images were compared with uncorrected respiratory motion average images. Results demonstrate that the use of elastic transformations in the reconstruction system matrix lead to uniform improvement across the lung field for different lesion sizes. The use of a trilinear interpolation or the incorporation of the b-spline functions lead to times of execution equivalent to standard image reconstruction. However, trilinear interpolation leads to artefacts in areas such as the diaphragm where the largest elastic deformations are occurring.**

Index Terms— **PET, respiratory motion correction, list-mode, image recontruction, elastic registration.**

I. Introduction

RESPIRATORY motion artefacts have been reported as a limiting factor of image quality and quantitation in PET thoracic imaging. In addition, the advent of combined imaging devices such as PET/CT, have placed extra emphasis on the need for respiratory motion correction. Potential methodology for reducing the effects of respiratory motion has been based on the development of respiration gated acquisitions leading to a number of frames corresponding to different parts of the respiratory cycle. However, the resulting gated images suffer from poor signal to noise ratio since each of the frames contain only part of the counts available throughout the acquisition of a respiration average PET dataset [1]. In an attempt to make use of all data available throughout a respiratory gated acquisition, we have previously developed and evaluated a method of incorporating elastic transformations in the system matrix during list-mode data based image reconstruction. This method was shown to provide significant improvements in terms of recovered activity concentration and position of pulmonary lesions [2]. However, one of the drawbacks of this implementation has been an increased time of execution. In order to improve in this aspect as well as on the accuracy, a new approach was developed using elastic transformations during the reconstruction process not only accounting for event misplacement as a result of respiration, but also for voxel deformation during reconstruction resulting from the use of elastic transformations. Finally, the different approaches of incorporating elastic transformations during the reconstruction process for respiratory motion correction in 4D PET/CT were compared.

II. Materials and Methods

A Monte-Carlo simulation study of the 4D NCAT phantom and two 4D PET/CT clinical studies were used in the validation of the new developed reconstruction algorithm. The simulated datasets were used in the quantitative comparison of the different approaches of incorporating elastic deformations in the reconstruction system matrix for respiratory motion compensation.

A. Simulation study

Simulated datasets were obtained using GATE (Geant4 Application for Tomographic Emission) [3]. The model of a clinical PET system previously validated by Lamare et al [4] was combined with the 4D NCAT phantom [5] in order to obtain dynamic emission frames acquired throughout

1-4244-0561-0/06/$20.00 ©2006 IEEE.

a respiratory cycle. A number of different size (7, 11, 15, 21mm) lesions were included at different locations throughout the lungs and the liver. Eight NCAT emission images were produced during a normal respiratory cycle of 5s. Finally, the simulated data corresponding to each individual frame was stored in list mode format.

B. Clinical study

4D PET/CT studies performed with the GE DST PET/CT scanner on two patients were used for a qualitative study of the correction methodology. PET data were acquired in list-mode format and subsequently binned in ten temporal frames of 500ms each, whereas 10 corresponding CT images were acquired during a respiratory cycle. The good correlation between CT dynamic images and the reconstructed non attenuation corrected PET emission images was visually verified.

C. Elastic transformation fields

For both clinical and simulation studies, the 4D CT images were used in combination with an elastic registration to define the transformation fields to be used during the reconstruction of the list mode emission data, except for the second patient in which case the gated PET images were used to derive the transformation fields. Deformation matrices were derived between all individual frames and that corresponding to full exhalation (i.e. frame 1). Elastic registration was performed using a spatio-temporal algorithm for motion reconstruction from a series of images [6]. This method uses a semi-local spatio-temporal parametric model for the deformation using B-splines and reformulates the registration task as a global optimization problem [7].

D. Implementation of the elastic transformation on the list mode data

The elastic motion correction has been integrated in a mathematical representation of the system matrix in the PET reconstruction process. If one notes A the system matrix usually describing the PET system, and whose elements a_{ij} represent the geometric probability of detecting at LOR i an event generated in voxel j, the data acquisition process can be represented by the equation:

$$m = Af \tag{1}$$

where m are the measured data sets, and f is the radioactive distribution. If t_0 corresponds to the reference frame time, and the matrix D_t represents the deformation of the radioactive distribution from time t to time t_0, the above equation becomes:

$$m_t = AD_t f \tag{2}$$

where m_t are the measured data sets at time t, and f remains the radioactive distribution had the object not moved (i.e corresponding to the reference frame time). The number of deformation matrices corresponds to the number of available CT dynamic frames.

This elastic based respiratory motion correction can be integrated in any iterative reconstruction process, based on either list mode or sinogram data, using a representation of the system matrix as described in equation 1. In our case, the One-pass list mode EM (OPL-EM) algorithm [8], combined with the accelerated version of the Siddon ray tracing [9], was implemented for the reconstruction of both simulated and clinical list-mode files:

$$f^{k+1} = \frac{f^k}{S} \int_{t_{acq}} {D_t}^T A^T \frac{1}{AD_t f^k} \tag{3}$$

where $.^T$ is the transpose operator, and t_{acq} is the overall acquisition time.

The sensitivity image S used to correct for attenuation and normalisation was equally modified to account for the motion correction:

$$S = \frac{1}{t_{acq}} \int_{t_{acq}} {D_t}^T A^T A_{atn} \text{ , with } A_{atn} = exp(-AD_t\mu) \tag{4}$$

μ is the linear attenuation coefficient for each voxel at the energy of 511keV.

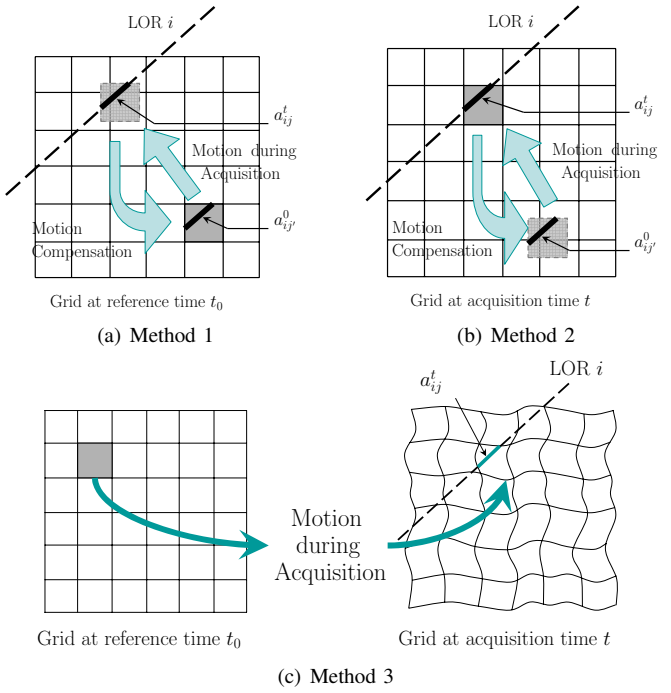

(a) Method 1 (b) Method 2

(c) Method 3

Fig. 1. Graphical representation of the three different methods of incorporation of the elastic motion compensation during recontruction, as described in section II.D: (a). method 1, (b). method 2, (c) method 3.

Three different implementations of the elastic transformation in the system matrix were compared (see figure 1):

1) Method 1: The matrix D_t contains the motion between a voxel of the grid at reference time t_0 and the acquisition time t. In this implementation, the actual position at time t doesn't necessary correspond to a voxel of the reconstruction grid. As a result the Siddon algorithm can't be used for the calculation of the system matrix. Therefore the exact coefficient a^t_{ij} is calculated [2], and no interpolation is required.
2) Method 2: The matrix D_t represents the motion between a voxel of the grid at acquisition time t and reference

frame time t_0. The computed coefficient a_{ij}^t corresponding to acquisition time t is therefore displaced to the reference time frame position (i.e $a_{ij'}^0$) and interpolated (trilinear interpolation based on the overlapping volumes of the 8 neighbouring voxels) to derive the coefficients [10].

3) Method 3: The matrix D_t contains the motion between a voxel of the grid at reference time t_0 and the acquisition time t, as well as the shape deformation of the voxels provided by the B-spline model of the elastic registration used to determine the motion correction parameters.

Four different reconstructions were performed:

- The first frame of the respiratory cycle, representing the reference image was reconstructed with the same count stastistics as for the entire respiratory cycle (*Frame1* image)
- The temporal frames were summed without any transformation and reconstructed (Respiratory *Average* image).
- Each of the three methodologies of implementing elastic transformations in the reconstruction system matrix described above were considered (respectively *Elastic1*, *Elastic2*, *Elastic3* images).
- In the case of the simulated datasets, each of the individual temporal gated frames were reconstructed. The images corresponding to the last frames were corrected using the same non-rigid registration parameters cited above, and were subsequently summed together. (*Gated-Frames* image).

E. Image analysis

In a quantitative fashion using the simulated datasets, the motion corrected images (*Elastic* and *Gated-Frames*) of the NCAT phantom were compared to the first temporal frame (reference image). The total number of coincidences were kept the same for all images in order to distinguish the effects purely associated with motion, rather than including those arising from differences in statistical quality between the single temporal frame (including only part of the data) and the corrected frames (including all of the available data). In order to better quantify motion compensation, we have also compared the two corrected images (*Elastic* and *Gated-Frames*) with the respiratory average image.

The contrast and FWHM improvements are computed as follows:

$$\%\ improvement = \left| \frac{Evaluated - Frame1}{Non\text{-}Corrected - Frame1} \right| \times 100 \quad (5)$$

where *Evaluated* can be either each of the three *Elastic* images or the *Gated-Frames* image.

To assess the improvement in terms of contrast in the reconstructed images, regions of interest (ROI) were placed in each of the lung lesions and in the background lung. The slice with the maximum count density over the lesion was identified for the ROI analysis. Average count densities were subsequently derived for each lesion.

On the other hand to quantify the position and "spreading" improvement as a result of the motion compensation, line profiles were drawn in the x, y and z directions for each lesion. Each of the lung lesion profiles was subsequently fitted with a gaussian in order to derive the position and FWHM in all three dimensions.

In a qualitative fashion using clinical datasets, profiles were plotted across regions of the FOV suffering from large respiratory motion effects.

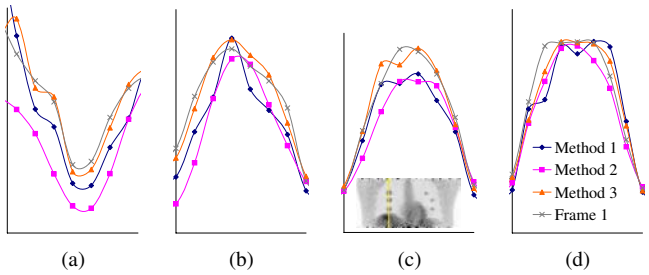

Fig. 2. Profile of the NCAT reconstructed images across (a). the edge of liver and (b-d). the lung lesion at the lower, middle, and upper part of the right lung respectively.

TABLE I

COMPARISON OF RAW BASED AND IMAGE BASED METHODOLOGIES IN TERMS OF BIAS IN THE ACTIVITY CONCENTRATION, POSITION AND SIZE OF THE DIFFERENT LUNG LESIONS, USING THE SIMULATED DATASETS.

% improvement	raw based methodology (*Elastic3* image)	image based methodology (*Gated-Frames* image)
bias	77% - 99%	62% - 88%
position	78% - 99%	37% - 87%
size	67% - 92%	24% - 87%

III. RESULTS

The closer agreement between the profiles of method 3 and gated frame 1 (figure 2) illustrates a higher accuracy obtained by accounting for the shape deformation of the voxels in the reconstruction process. Figure 3(c), 3(d) and 3(e) demonstrate differences in terms of image quality between the three different implementations of elastic transformations based image reconstructions using the simulated NCAT frames. Low uptake areas can be observed in the diaphragm using the reconstruction method 2 as a result of a combination of significant elastic deformations in this region and not accounting for the voxel shape deformation associated with the elastic transformation process. The artefacts originating as a result of the use of the trilinear interpolation can be clearly also observed in figures 4 and 5 showing the results obtained for the patient studies. Similar reconstruction times were observed for methods 2 and 3, while method 1 was slower by approximately a factor of ten.

Table I contains the results on a comparison of the incorporation of the elastic deformations during the reconstruction process and that of applying the deformation fields in the reconstructed gated images which can be subsequently summed together. These results demonstrate an improvement of ∼62-99% in terms of contrast on lung lesions in the corrected images depending on lesion location and size. A larger

improvement was generally observed for smaller lesions, although the 7mm lesion results suffer from significant partial volume effects. Same results can be observed in terms of position and size of the different size lung lesions. In addition, the corrected images using the reconstruction proposed as *Method3* lead to more uniform results and improvements for all the three considered criteria in comparison to the image based methodology.

IV. Discussion

The solutions that have been proposed to date for taking into account the effects of respiratory motion concentrate on the acquisition of respiration synchronised PET and CT datasets. Irrespective of the gating methodology implemented the emission data acquired in each of the temporal gated frames is reasonably free of respiration produced inaccuracies. However, the resulting individual frame images are of reduced resolution as well as overall quality as they contain only a fraction of the counts available throughout a PET acquisition. Therefore the need exists for the development of correction methodologies, making use of the gated datasets, in order to obtain respiration free PET images using all available data throughout a standard respiration average PET acquisition. This approach will also remove the need currently existing in terms of significantly increasing the time (over a factor of 3) of gated PET acquisitions in order to compensate for the presence of reduced statistics in the final reconstructed images. Very limited work is currently available in this domain. Our objective in this study has been to assess the improvement that can be obtained in terms of lesion contrast and location as a result of correcting gated raw list mode datasets for the presence of respiratory motion through the application of an elastic transformation during the reconstruction process.

Our study was based on the use of the NCAT phantom with the introduction of variable size and location lesions in the lung field and in the liver in order to assess quantitative improvements. This method was also validated with two clinical cases. Elastic transformation fields were derived by using either the 4D CT attenuation maps or the gated PET frames. The OPL-EM algorithm was adapted to integrate the elastic transformation during the reconstruction process. Dedicated attenuation and normalisation corrections were also developed to take into account the applied elastic transformation.

The implementation of the elastic transformation during the image reconstruction process is based on the incorporation of the necessary deformations in the system matrix. During such deformations the contribution of voxels is shifted to a new position in the reconstruction grid accounting for the effects of movement. The problem is that the new location of the voxel does not coincide to a voxel in the reconstruction grid. Subsequently pre-calculated probabilities for the sensitivity matrix cannot be used, leading to considerable increases in the reconstruction time of execution [2]. One way to overcome this issue is the use of a trilinear interpolation based on the overlap of the volume of the displaced voxel to that of the eight neighbouring voxels of the reconstruction grid over which it is moved as a result of the predetermined transformation [10]. Although this approach allows the use of pre-calculated sensitivity matrix probabilities it does not account for the change in the voxel shapes as a result of the non-rigid nature of the deformations involved. Such distortions are generally larger in the areas where the elastic deformations are more significant, such as for example in the area of the diaphragm. We have proposed and evaluated in this work the direct use of b-spline functions in order to account for these voxel distortions.

As figures 3(d) and 4(c) demonstrate white band artefacts appear due to the use of trilinear interpolation, particularly in the region of the diaphragm where the elastic deformations associated with the lungs and the organs below the diaphragm such as the liver and the stomach is most significant. In the case of the second patient, the FOV is not at the level of the diaphragm limiting in such way the severe artefacts observed in the first clinical case. By taking into account the elastic deformations involved by the respiratory motion through the use of the b-spline functions in the reconstruction sensitivity matrix all such artefacts are eliminated as demonstrated in the simulated (figure 3) and clinical cases (figures 4, 5).

The results obtained at that stage of our investigation allowed us to predict a considerable improvement in the lung and cardiac fields through the application of an elastic transformation.

The incorporation of the elastic deformations in the reconstruction process was also compared with an image based respiratory motion correction where the elastic transformations are applied after the reconstruction of the individual gated frames. As the quantitative analysis of the simulated results has demonstrated the raw data based approach leads to superior results in terms of improvement in lesion size, location and contrast in comparison to the image based correction.

V. Conclusions

Three different methods of implementing elastic transformation during image reconstruction were compared and their performance evaluated on simulated and clinical emission datasets. A comparison of the reconstructed images reveal that accounting for voxel shape deformation as a result of the elastic transformation improves significantly image quality, particularly in the areas where respiratory motion is most significant.

References

[1] L. Boucher, S. Rodrigue, R. Lecomte *et al*, *Respiratory gating for 3D PET of the thorax: feasibility and initial results*, J Nucl Med, 45, 214-219, 2004.

[2] F. Lamare, M.J. Ledesma Carbayo, G. Kontaxakis *et al Incorporation of Elastic Transformations in List-Mode Based Reconstruction for Respiratory Motion Correction in PET* IEEE MI conference records 2005.

[3] S. Jan, G. Santi, D. Strul *et al*, *GATE: a simulation toolkit for PET and SPECT*, Phys. Med. Biol, 2004, 49, 4543-4561

[4] F. Lamare, A. Turzo, Y. Bizais,D. Visvikis *Validation of a Monte Carlo simulation of the Philips Allegro/GEMINI PET systems using GATE*, Phys. Med. Nucl., 51, 943-962, 2006.

[5] W.P. Segars, D.S. Lalush, B.M.W Tsui, *Modelling respiratory mechanics in the MCAT and spline-based MCAT phantoms*, IEEE Trans Nuc Sc, 48(1), 89-97, 2001.

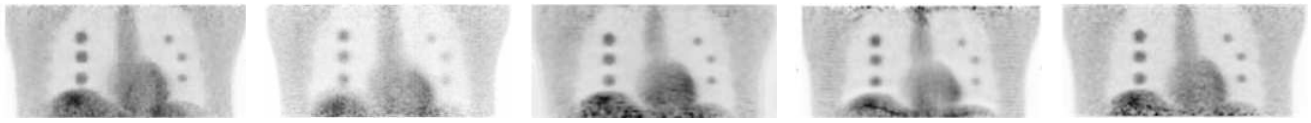

(a) (b) (c) (d) (e)

Fig. 3. List-Mode simulated emission data sets of the NCAT phantom reconstructed with: (a). frame 1 (reference image), (b). respiratory average image, (c). method 1, (d). method 2, (e) method 3.

(a) (b) (c) (d)

Fig. 4. List-Mode emission data sets of the first patient reconstructed with: (a). frame 1 (reference image), (b). respiratory average image, (c). method 2, (d). method 3.

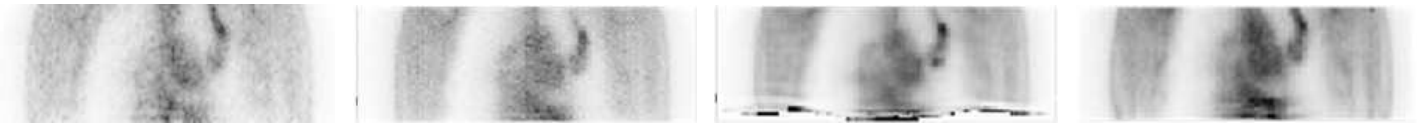

(a) (b) (c) (d)

Fig. 5. List-Mode emission data sets of the second patient reconstructed with: (a). frame 1 (reference image), (b). respiratory average image, (c). method 2, (d). method 3.

[6] M.J Ledesma-Carbayo, J. Kybic, M. Desco, A. Santos, M. Suhling, P. Hunziker, M. Unser, *Cardiac motion analysis from ultrasound sequences using non-rigid registration* IEEE Trans Med Imag, 1113-1126, 2005

[7] D. Visvikis, M. Leesma-Carbayo, F. Lamare *et al A spatiotemporal image registration algorithm for respiratory motion correction in PET/CT*, J Nucl Med, 2006, in press

[8] A.J. Reader, S. Ally, F. Manavaki, R.J. Walledge, A.P. Jeavons *et al One-pass list-mode EM algorithm for high-resolution 3D PET image reconstruction into large array*, IEEE Trans Nucl Sci, 49(3), 693-699, 2002.

[9] G. Han, Z. Liang, J. You *A fast Raytracing Technique for TCT and ECT Studies*, IEEE MI Conference records, 1999.

[10] F. Qiao, T. Pan, J.W. Clark, O.R. Mawlawi *Compensating Respiratory Motion in PEt image Reconstruction using 4D PET/CT*, IEEE MI Conference records, 2005.